THE JOURNAL OF COMPARATIVE NEUROLOGY 440:271–283 (2001)

# Tiling of the Body Wall by Multidendritic Sensory Neurons in *Manduca sexta*

**WESLEY B. GRUEBER,* KATHERINE GRAUBARD, AND JAMES W. TRUMAN**
Department of Zoology, University of Washington, Seattle, Washington 98195

ABSTRACT

A plexus of multidendritic sensory neurons, the dendritic arborization (da) neurons, innervates the epidermis of soft-bodied insects. Previous studies have indicated that the plexus may comprise distinct subtypes of da neurons, which utilize diverse cyclic 3′,5′-guanosine monophosphate signaling pathways and could serve several functions. Here, we identify three distinct classes of da neurons in *Manduca*, which we term the *alpha*, *beta*, and *gamma* classes. These three classes differ in their sensory responses, branch complexity, peripheral dendritic fields, and axonal projections. The two identified alpha neurons branch over defined regions of the body wall, which in some cases correspond to specific natural folds of the cuticle. These cells project to an intermediate region of the neuropil and appear to function as proprioceptors. Three beta neurons are characterized by long, sinuous dendritic branches and axons that terminate in the ventral neuropil. The function of this group of neurons is unknown. Four neurons belonging to the gamma class have the most complex peripheral dendrites. A representative gamma neuron responds to forceful touch of the cuticle. Although the dendrites of da neurons of different classes may overlap extensively, cells belonging to the same class show minimal dendritic overlap. As a result, the body wall is independently tiled by the beta and gamma da neurons and partially innervated by the alpha neurons. These properties of the da system likely allow insects to discriminate the quality and location of several types of stimuli acting on the cuticle. J. Comp. Neurol. 440: 271–283, 2001. 

**Indexing terms: peripheral nervous system; Lepidoptera; dendrite; morphogenesis mechanoreceptor**

*Tiling* refers to the complete, but nonredundant, innervation of an area or surface by neuronal dendrites. Tiling occurs between functionally similar neurons, such that each cell has its own dendritic field that does not overlap with those of like neurons. Consequently, the flow of information from tiled systems is efficient, and its location of origin is unambiguous. One well-established example of tiling occurs among the alpha ganglion cells of the vertebrate retina (Wässle et al., 1981). Alpha cells show OFF-center or ON-center responses to light stimuli. OFF neurons and ON neurons independently tile the retina with dendrites and, therefore, provide complete samplings of the receptive area (Wässle et al., 1981). Tiling of retinal ganglion cells has important implications for the detection of visual information (Amthor and Oyster, 1995) and also the development of neuronal ensembles (Perry and Linden, 1982; Weber et al., 1998).

Tiling could also be an efficient way to organize mechanosensory neurons, which must have defined and unique receptive fields to convey the location of stimuli. For example, touch-sensitive, pressure-sensitive, and nociceptive neurons of the leech show some evidence of tiling. Each neuron projects to a specific region of the hypodermis, where it forms a defined receptive field (Nicholls and Baylor, 1968; Blackshaw, 1981). Interactions between branches influence receptive field overlap among cells of the same modality (Blackshaw et al., 1982; Gan and Macagno, 1995). Tiling may also occur in an insect somatosensory system. Bilaterally homologous dorsal dendritic arborization (da; Bodmer and Jan, 1987) neurons in *Drosophila* larvae are excluded from each other's dendritic

Contract grant sponsor: National Institutes of Health; Contract grant number: NS 13079; Contract grant sponsor: National Institute of General Medical Sciences; Contract grant number: PHS NRSA T32 GM07270; Contract grant sponsor: UW ARCS Fellowship.

*Correspondence to: Wesley B. Grueber, Departments of Physiology and Biochemistry, Howard Hughes Medical Institute, 533 Parnassus Avenue, Room U226, University of California, San Francisco, CA 94143-0725. E-mail: grueber@itsa.ucsf.edu

Received 14 June 2001; Revised 21 August 2001; Accepted 27 August 2001

fields (Gao et al., 2000). The morphologies and functions of individual da neurons have not been established in *Drosophila*, so it is not clear how neurons of the same type establish their dendritic fields.

In *Manduca* and *Drosophila*, there are 12–16 identifiable da neurons in each abdominal hemisegment, arranged in a stereotypic pattern on the epidermis (Bodmer and Jan, 1987; Grueber and Truman, 1999). These neurons spread extensive overlapping dendritic branches across the entire body wall. A distinct and more abundant group of da neurons, the secondary plexus cells, are seen in *Manduca* but not in *Drosophila* (Grueber and Truman, 1999). No studies have directly examined the physiology of larval da neurons, but their axonal projections in *Drosophila* indicate that they could sense several different types of mechanical stimuli (Schrader and Merritt, 2000). Diverse functions for the da neurons are also suggested by the selective expression of *pickpocket* (*ppk*), a degenerin/epithelial $Na^+$ channel thought to be involved in mechanotransduction, in only a subset of the neurons (Adams et al., 1998; Darboux et al., 1998). Furthermore, in *Manduca* larvae, two da neurons exhibit $Ca^{2+}$-sensitive production of the second messenger cyclic 3′,5′-guanosine monophosphate (cGMP), whereas all others show nitric oxide-induced cGMP production (Grueber and Truman, 1999). The diverse functions of the da system might be better understood by examining the morphology and arrangement of individual neurons.

Here, we examine the functional and morphological properties of the da system of *Manduca sexta*. We identify, among the identifiable da neurons, three distinct morphological and functional types of cells, which we term the *alpha*, *beta*, and *gamma* classes. The beta and gamma neurons tile the epidermis with dendrites, whereas alpha neurons send selective projections to specific regions of the body wall. We discuss the functional and developmental implications of these findings and provide a framework for understanding the diverse cGMP signaling pathways in the *Manduca* da system.

## MATERIALS AND METHODS

### Animals

*Manduca sexta* larvae were raised in individual containers on an artificial diet (Bell and Joachim, 1976) on a 16L:8D photoperiod. For staging nomenclature, ecdysis (shedding of the old cuticle) marks the beginning of day 0 for a given stage.

### Electrophysiology

We recorded from da neurons in an isolated body wall preparation. After immobilizing day 0 fifth-instar *Manduca* larvae on ice, they were immersed in fresh saline (Weevers, 1966a; Trimmer and Weeks, 1989). A longitudinal incision was made, and the majority of fat body and muscles were removed to expose the subepidermal neurons. To minimize the contribution to nerve activity made by neurons other than the da cells, we transected all of the sensory nerve branches except for those originating from the dorsalmost region of the segment. Consequently, only activity from dorsal da neurons and dorsal sensory bristles were observed in our recordings. We found that a high-$Na^+$ saline was advantageous when suction electrodes were placed on the proximal regions of the dorsal nerve. The use of normal high-$K^+$ saline (Weevers, 1966a,b) caused a gradual and reversible decline in unit amplitude, although the units remained at approximately the same frequency when recordings were made near the sensory cell bodies. The sensitivity to high-$K^+$ saline may result from the stretching of the dorsal nerve during dissection (and, hence, partial disruption of the blood–brain barrier; Pinchon et al., 1972) or from $K^+$ leakage into the nerve through the transected lateral branches. We mounted the preparation cuticle side up on two Sylgard blocks and recorded from the proximal end of the dorsal nerve using suction electrodes.

Stimuli were applied by hand for approximately 0.5 seconds via a series of Semmes-Weinstein von Frey monofilaments (Stoelting, Wood Dale, IL). We measured the average bending force of each filament using a force transducer (constructed by Dr. M. Tu, University of Washington) and multimeter. For receptive field mapping, the entire region of the segment examined was draped over a Sylgard block, and stimuli were applied for approximately 0.5 seconds at 30–40 second intervals. For examining the responses to graded stimuli, only the stimulated region of a segment was placed over the block, and stimuli were applied at 1 minute intervals. All recordings were made within 1 hour of completing the dissection. Traces were recorded on a Mitsubishi HSU430 VCR and transferred to a Macintosh computer (Apple Computer, Cupertino, CA) at 10,000 samples/second using Superscope 2.12 (GW Instruments).

### Dye fills

Hatchling and day 0 second-instar larvae were pinned flat on a Sylgard dish (Dow Corning, Midland, MI) and covered in modified Miyazaki's saline (in mM: NaCl, 130; KCl, 5; $CaCl_2$, 4; glucose, 28; HEPES, 5; pH 7.4; Miyazaki, 1980; Trimmer and Weeks, 1989) or Weevers' larval saline (in mM: NaCl, 12; KCl, 30; $MgCl_2$, 18; $CaCl_2$, 3; glucose, 133; $NaHCO_3$, 1.5; $NaH_2PO_4$, 1.5; pH 6.4; Weevers, 1966a). Larvae were then dissected along the lateral body wall, and fat body and muscles were carefully removed to expose the epidermis with its supply of sensory neurons. Quartz microelectrodes pulled on a Sutter P-2000 laser electrode puller (Sutter Instruments, Novato, CA) were backfilled with 4% Lucifer yellow (LY; Molecular Probes, Eugene, OR) in 0.1 M LiCl, and the shafts were filled with 1 M LiCl. Neurons were identified with transmitted light under 250× magnification, impaled, and filled using intermittent high-frequency voltage oscillations of the electrode (buzzing), applied from an Axoclamp 2A microelectrode amplifier (Axon Instruments, Foster City, CA). The progress of the filling was occasionally monitored using brief fluorescent illumination. Once filling was complete, the tissue was fixed for 1 hour in 4% formaldehyde in phosphate-buffered saline (PBS), pH 7.4, dehydrated in ethanol series (5 minutes each in 30%, 50%, 70%, 95%, 100%, 100%), cleared in xylene, and mounted in DPX (Fluka, Milwaukee, WI). For double dye fills, one cell was filled with LY as described above and the other via a microelectrode with a tip that was filled with 4% biocytin/2% sulforhodamine 101 (Sigma, St. Louis, MO) in 0.5 M KCl and a shaft filled with 3 M KCl. Sulforhodamine was included to determine at the time of filling whether a cell fill was successful. After fixation in 4% formaldehyde, preparations were blocked in normal donkey serum (NDS) and incubated in 1:200 rabbit anti-LY (courtesy of Dr. J.

Kuwada) and 1:200 avidin-Texas red (Jackson Immunoresearch, West Grove, PA) overnight at 4°C. These preparations were rinsed for several hours and then incubated overnight in 1:1,000 fluorescein isothiocyanate (FITC)-conjugated donkey anti-rabbit (Jackson Immunoresearch). Our analyses of the peripheral arborization patterns are based on an "idealized" abdominal segment, the second abdominal segment (A2). The da neurons occupy ventral, lateral, and dorsal positions on the body wall. The arrangement of dorsal neurons is invariant in A2–A6, so they were filled in any of these segments. The arrangement of ventral neurons varies in A3–A6 because of the presence of prolegs (Grueber and Truman, 1999), so we restricted our analysis of ventral neurons to those of A2.

### Image processing

Cell fills were viewed using a Bio-Rad MRC-600 confocal microscope (Bio-Rad, Hercules, CA) equipped with a 40×, 1.3 N.A. oil-immersion lens (Olympus). Z-series projections were made using COMOS software (Bio-Rad, Hercules, CA) and reconstructed into montages (Beck et al., 2000) using Adobe Photoshop 5.0. The "levels" command was used to equalize the black levels of the various pieces of the reconstructed images. Figure 5B was modified to mask the cell body of a single neuron, dorsal dendritic arborization D (ddaD), which was partially filled and whose presence obscured some of the dendrites of ddaC. Computer tracings of dendritic arbors were made in Photoshop by using the "layers" function and tracing the arbors by mouse. Dorsoventral views of da axonal projections within the central nervous system (CNS) were made using NIH Image 1.62 (available at http://rsb.info.nih.gov/nih-image) by projecting confocal Z-series files (1.0 μ steps) 90° around the x-axis, with four pixels spaced between each of the z-sections (1 pixel = 0.265 μm; final distance between sections = 1.06 μm).

### Quantification of dendritic complexity

We used the Strahler method (Strahler, 1953; Uylings et al., 1975) to order and analyze systematically the dendritic branches of da neurons. In this method, terminal branches are assigned an order of 1. The meeting of two first-order branches creates a new order 2. Where two second-order branches meet, an order of 3 is created, and so on. If a lower order branch (i.e., 2) meets a higher order branch (i.e., 3), the higher order branch is carried on unaffected. Once dendrites were ordered in such a manner, the magnitudes were transformed into a reversed Strahler order in which the main branches exiting the soma are assigned an order of 1, the next an order of 2, and so on to the terminal branches (Berry et al., 1975).

## RESULTS

### Organization of *Manduca* da neurons

Grueber and Truman (1999) described the anatomical organization of the *Manduca* peripheral nervous system (PNS). Depending on the body segment, there are 12–16 large, multidendritic da neurons per hemisegment, and these occupy characteristic positions along the epidermis (Fig. 1). The positioning of the cells is reflected in their nomenclature (vda, ventral da neuron; lda, lateral da; and dda, dorsal da; Grueber and Truman, 1999). Each name is also suffixed with a unique identifier, generally an upper-case alphabetic, indicating the typical order in which the neuron is encountered from ventrally to dorsally and anteriorly to posteriorly along the hemisegment. Collectively, the dendrites of these da neurons overlap extensively and provide redundant coverage of the entire trunk of the animal. A second set of da neurons, the secondary plexus neurons, is generated as a component of external sensory bristle lineages and is distributed in columns across the body wall (Grueber and Truman, 1999). These columns correspond to the eight annuli evident in the dorsal and lateral regions in each abdominal hemisegment. Because the secondary cells are smaller, more numerous, and not uniquely identifiable, we do not treat them further here. Instead, we focus exclusively on the larger, identifiable, da neurons (Fig. 1).

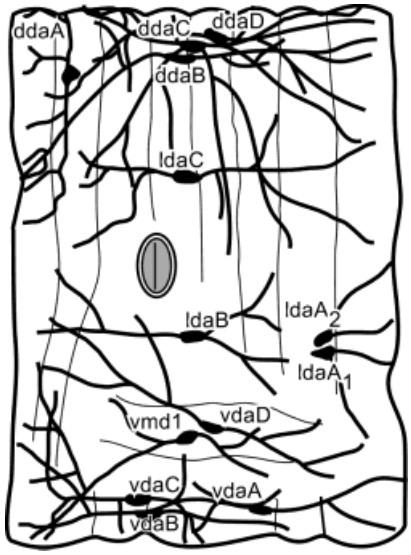


Fig. 1. Schematic drawing of the arrangement of multidendritic dendritic arborization (da) neurons that make up the second abdominal hemisegment of *Manduca sexta*. The oval indicates the position of the spiracle. Note the eight annuli that subdivide the segment. Anterior is to the left and dorsal is upward.

### Electrical activity of dorsal da neurons

To gain insight into the possible functions of da neurons, we measured the afferent discharge of ddaB, ddaC, and ddaD, three neurons whose cell bodies cluster together in the dorsal body wall (see Fig. 1). Suction electrode recordings from the nerve, containing the axons of these three cells, revealed two consistent units in fifth-instar larvae, a small amplitude unit with a highly regular basal activity and a larger amplitude unit with an irregular, low-frequency basal activity (Fig. 2A). Each unit appeared to correspond to a single cell, in that same-sized spikes were not superimposed even during cuticle stimulation (see below). Similar basal activity was observed in first- and fourth-instar preparations (data not shown), but fifth-instar larvae were better suited for further electrophysiological studies because of their large size. To narrow down the identities of the neurons responsible for the two units, we performed cutting experiments and cell ablations. Crushing the cell body of ddaD or cutting the nerve containing its axon eliminated the large-amplitude unit in 12 of 17

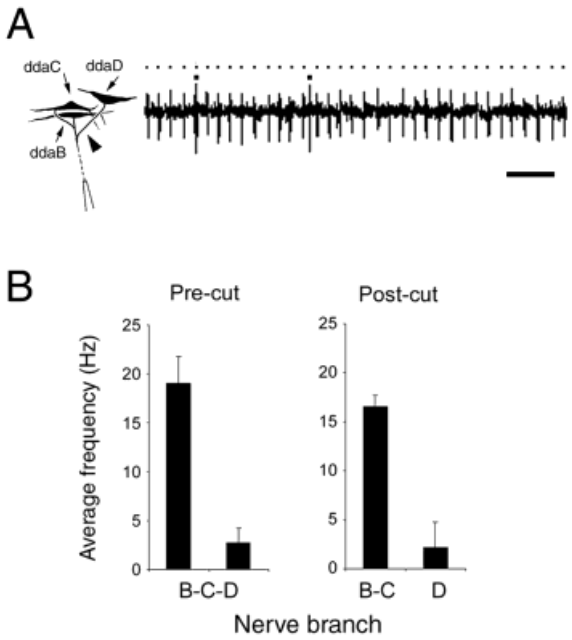


Fig. 2. Identifications of electrical activity of dorsal dendritic arborization (da) neurons. **A:** Recordings from the dorsal nerve in day 0 fifth-instar larvae reveal two units, a small unit that fires at a relatively high frequency (upper dots) and a large unit with irregular activity (lower dots). **B:** Comparisons of the average frequencies before and after transection of the branch leading to ddaD (n = 4; the point of transection is indicated by an arrowhead in A). Shown are the average frequencies ± SD of each nerve trunk from one representative transection. Left: Prior to the branch cut, high-frequency and low-frequency units are observed. Right: After transection, the high frequency unit is observed from the ddaB,C branch and a low-frequency unit in the ddaD branch. B-C-D, nerve branch with ddaB, ddaC, and ddaD axons; B-C, nerve branch with ddaB and ddaC axons; D, nerve branch with ddaD axon. Scale bar = 100 msec.

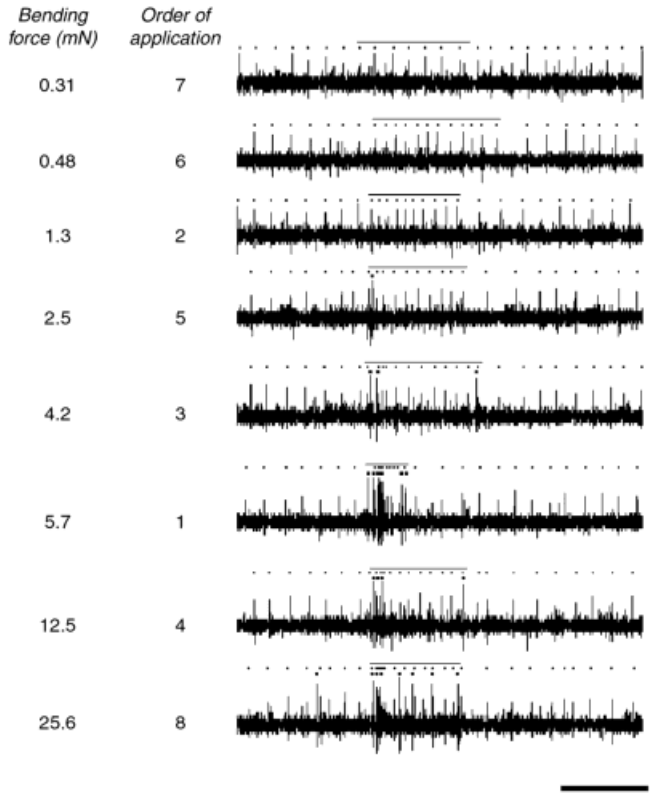


Fig. 3. Responses of dendritic arborization neurons to punctate stimuli. A graded series of von Frey monofilaments ranging from ~0.3 mN to ~26 mN was applied to the dorsal posterior cuticle in random order. Stimuli were delivered 1 minute apart in the order indicated. Responses were monitored with an extracellular suction electrode. A bar above each trace indicates the period of stimulation. The uppermost row of dots above each trace indicates the firing pattern of the smaller unit; the lower row of dots indicates firing of the larger unit. The small unit shows a response to filaments of approximately 0.5 mN and above throughout the period of stimulation. The 0.5 mN filaments caused a local deformation of the cuticle. The larger unit fires at the beginning of each stimulus when the filament strength reaches 2.5 mN, a force sufficient to press the cuticle against the recording dish. At 4.2 mN and above, this unit begins firing also at the end of each stimulus and at 25.6 mN fires throughout the period of stimulation, although at a lower frequency than it does at stimulation onset. Expansion of the traces indicated that the smaller spike-like units were likely electronic noise. Scale bar = 0.5 sec.

cases (70%). In four cases, the results were ambiguous (i.e., we could not determine whether the large-amplitude unit had decreased in size or whether the small-amplitude unit became irregular), and, in one case, neither unit was lost. In no case was the small-amplitude unit lost. After the nerve cuts, we recorded separately from the branch containing the ddaB/ddaC axons and that containing the ddaD axon (n = 5). The B-C branch contained a single unit with a steady, high frequency, whereas a large unit in the D branch fired at a lower, irregular frequency (Fig. 2B). Because the cell bodies of ddaB and ddaC lie immediately adjacent to one another, we could not ablate one cell without possibly damaging the other. These experiments, therefore, support the assignment of the larger unit as ddaD and the small high-frequency unit as either ddaB or ddaC.

Because the da neurons are thought to function as mechanoreceptors, we used a series of von Frey filaments of graded bending force to apply punctate stimuli to the cuticle. The small unit showed an increased frequency of firing in response to an indentation of the cuticle caused by filaments of ≥0.5 mN (Fig. 3). This unit adapted slowly and exhibited a brief poststimulus inhibition (Fig. 3). During more intense stimulation, the unit showed a high-frequency phasic response at the onset of the stimulus and a subsequent lower frequency response as long as the filament was held against the cuticle (Fig. 3). The larger amplitude second unit was activated by filaments of ≥2.5 mN (Fig. 3), which corresponded to those that were able to push the epidermis into the underlying Sylgard block. This cell showed a phasic response during the application and removal of each monofilament (Fig. 3). At higher stimulus intensities (≥25 mN), the cell also fired at a low frequency throughout the period of stimulation (Fig. 3). Thus, these two dorsal neurons show distinct responses to punctate stimuli.

We mapped the receptive field boundaries of the two units using a von Frey filament (4.2 mN average bending force; n = 4 animals). The small-amplitude unit showed the strongest responses within a dorsal strip of cuticle extending from the second to the fifth annulus (Fig. 4). Responses declined with distance from this region except

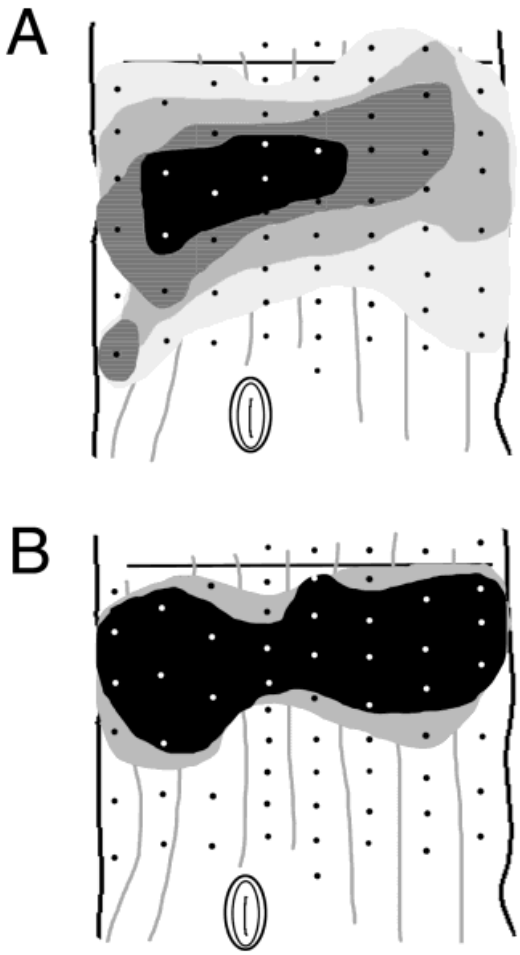


Fig. 4. Receptive fields of the dorsal da neurons. **A:** Receptive field mapping of the high-frequency unit using a 4.2 mN von Frey monofilament. Each point of stimulation is marked with a black or white dot. The responses of the nerve were monitored using a suction electrode. Shown are the responses from a single animal. The mappings were highly reproducible for each animal (n = 4; data not shown). Stimuli given within the same shade of gray produced similar increases in tonic firing frequency. Response categories from lightest to darkest (in Hz above background firing frequency): 0–2.4, 2.5–9.9, 10–29.9, 30–50. **B:** Receptive field of the phasic unit. Stimulation of the black areas caused high-frequency responses consisting of at least four consecutive spikes. Stimulation of the gray areas caused a brief 2–4 Hz increase in the constitutive firing rate. The oval indicates the position of the spiracle; a horizontal bar shows the location of the dorsal midline. Dark vertical lines are segment borders, and lighter lines are annulus borders.

for a small patch of cuticle in a more lateral region of the first annulus (Fig. 4A). The large-amplitude unit showed strong phasic responses from the first to the eighth annuli. The receptive field never crossed the dorsal midline and extended for about half the distance from the dorsal midline to the spiracle (Fig. 4B).

## Dendritic fields of the dorsal cluster of da neurons

To determine whether the dendritic fields of any of the dorsal da neurons corresponded to the areas that were mapped by von Frey hair stimulation, and to examine the morphological features of the dorsal da neurons, we made intracellular dye fills in first-instar larvae with Lucifer yellow and biocytin. We observed highly stereotyped peripheral branching patterns for ddaB, ddaC, and ddaD (n = 36, 19, 33, respectively; Fig. 5). Each cell differed considerably in its peripheral dendritic morphology: ddaB had sparse dendrites, with highly stereotyped projections and branch points; ddaC showed sinuous dendrites and uniform coverage of its territory; and ddaD showed a complex, highly branching arborization. We discuss the major features of each neuron below.

ddaB extended two major dendritic trunks over the segment in anterior and posterior directions. Each of these arbors made selective associations with particular regions of the hemisegment: The anterior trunk arborized primarily within the second annulus of each hemisegment, whereas the posterior trunk had sparse coverage of the more posterior annuli (Fig. 5A). A prominent feature of ddaB was an anterior arbor that extended beyond the second annulus and was associated with a lateral fold of the cuticle near the segment border (Fig. 5A). When the anterior region of the segment was stretched along the dorsoventral axis, the terminal arbors adopted a "fanned" appearance (Fig. 5A). The remaining branches of ddaB terminated in regions lacking visible cuticular specializations. Many of these branches were merely small stubs originating from the major trunks (Fig. 5A). Overall, the shape of the dendritic field of ddaB overlapped the receptive field of the small-amplitude tonic unit (see Fig. 4A). The anteriormost arbor was located at the local "hot spot" of activity observed in the mapping experiments (cf. Figs. 4A and 5A).

In contrast to the selective arborization of ddaB, the dendritic arbor of ddaC covered nearly the entire region of the hemisegment dorsal to the spiracle (Fig. 5B; n = 19). Primary dendrites showed a laminar radiation from the cell body and resolved into longer midorder dendrites that spread uniformly over the epidermis without overlapping each other (Fig. 5B). Dendrites terminated abruptly at the lateral margin of the segment at the level of the spiracle. The branches of ddaC failed to invade completely the most anterior and posterior regions of each hemisegment. At these margins, the dendrites often made sharp turns in dorsal or ventral directions. Such a morphology suggests that an avoidance signal other than the segment border may exist for ddaC in these anterior and posterior regions of the segment. The dendritic field of ddaC did not correspond to either of the receptive fields mapped for the dorsal units (cf. Figs. 4 and 5B).

The peripheral arbors of ddaD branched more extensively than either ddaB or ddaC (n = 33; Fig. 5C) and showed the highest complexity according to Strahler analysis (Table 1). Dendrites of ddaD extended over the entire anteroposterior length of a hemisegment but covered only the dorsalmost half of the area dorsal to the spiracle. As was the case with the other dorsal da neurons, the dendrites of ddaD did not cross the dorsal midline. The density of branching was high within each of the eight segmental annuli, but isoneuronal (same cell) overlap was not observed (Fig. 5C). The ramifications of a given branch were typically confined to a single annulus, and dendrites avoided terminating near annulus boundaries. Toward the segment borders, though, higher order branches occasionally crossed boundaries and terminated in adjacent annuli (Fig. 5C). The overall shape of the dendritic arbor

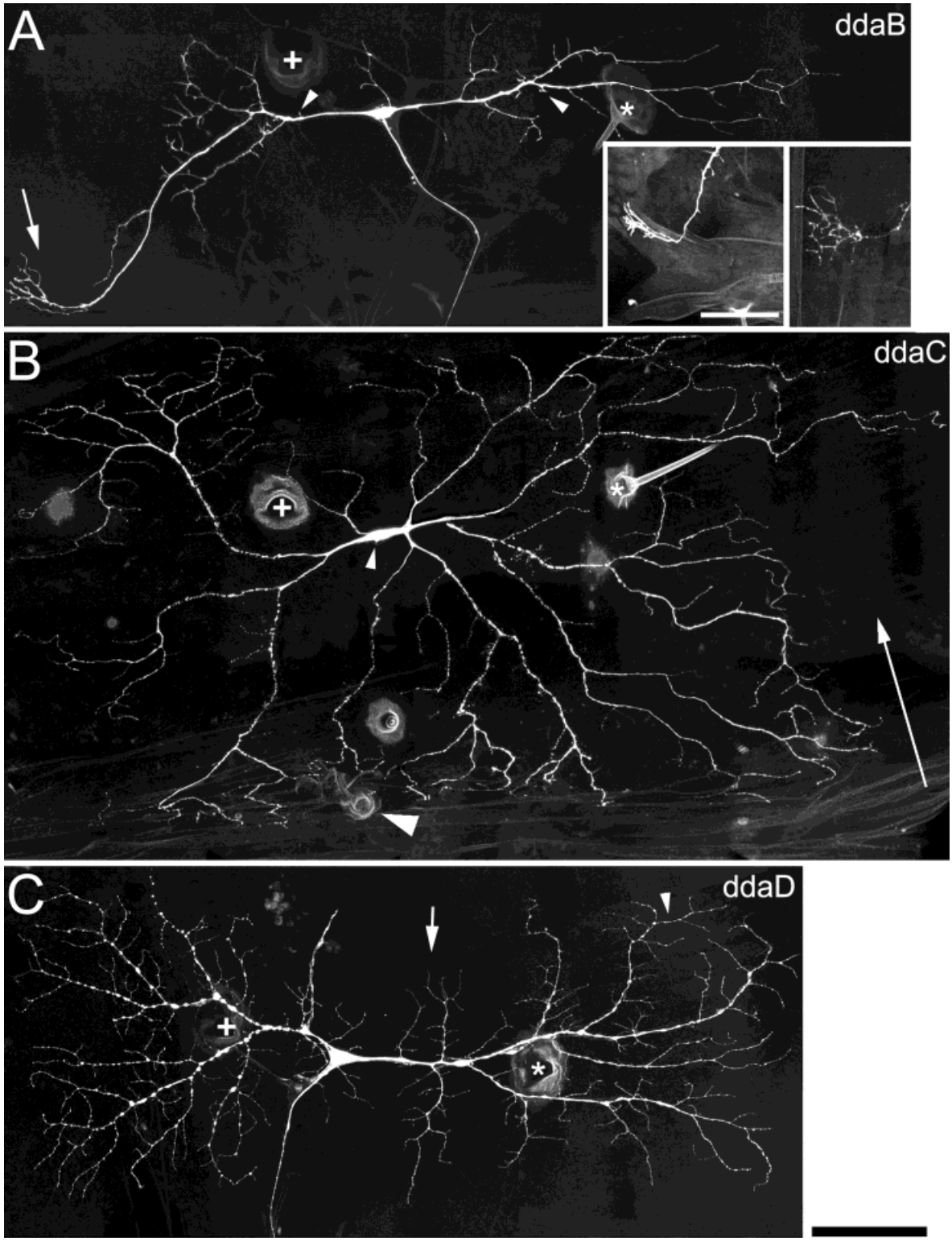


Fig. 5. Lucifer yellow fills reveal distinct dendritic patterns for dorsal dendritic arborization (da) neurons in first-instar larvae. Shown are confocal montages of ddaB (A), ddaC (B), and ddaD (C). Each neuron spans nearly the entire anteroposterior length of a segment. **A:** The dendrites of ddaB lack the conspicuous varicosities, or beads, seen in the other neurons and make terminations in selective regions of the body wall. Arrowheads show some of the many small knobs located on larger trunks. The axon of ddaB can be seen projecting ventrally toward the CNS. The spiracle is out of view at the bottom of the panel. **Inset:** Two cell fills showing the anterior dendritic arbor of ddaB (arrow in A) associated with a folded region of the lateral body wall (left) and the extension of this arbor after stretching of the cuticle (right). **B:** The dendritic field of ddaC covers nearly the entire dorsal half of the segment. This neuron has relatively long branching dendrites. The arrow points to a posterior margin (most of annulus 8) that is left void of dendrites. The axon was severed in this preparation; all that is visible is a small stump on the lower side of the cell body (small arrowhead). The spiracle is indicated by a large arrowhead. The cell body of ddaD was partially filled in this preparation and was digitally masked to reveal the full arbor of ddaC. **C:** ddaD covers only about half of the area of ddaC and extends to both segment borders. The major branches of ddaD correspond to the segmental annuli that ring the body wall (one branch innervating annulus 5 is denoted by an arrow). Some terminal branches were observed to cross annular boundaries before ending (arrowhead). The axon of ddaD can be seen extending from the cell body in a ventral direction. The spiracle is out of view at the bottom of the panel. The cell bodies of these three neurons cluster close together: For reference, the autofluorescent desB sensory bristle (plus signs; Grueber and Truman, 1999) is centered in annulus 3, and desC(2) is seen posterior to each cell body centered in annulus 6 (asterisks). Anterior is to the left and dorsal is upward in all images. Scale bars = 100 μm.

of ddaD matched the receptive field of the large-amplitude unit (see Fig. 4B).

These morphological data, together with the electrophysiology and cell ablation experiments, suggest that ddaB is responsible for the small unit that shows both phasic and tonic responses to mechanical deformation of the cuticle. ddaD, on the other hand, is the larger unit that gives a phasic response to more intense punctate stimuli. Because we could not identify a unit that corresponded to ddaC, we do not know its sensory role.

TABLE 1. Reversed Strahler Analysis of Dendritic Arborization Neurons in First-Instar Larvae

| | | Branch order[1] | | | | |
|---|---|---|---|---|---|---|
| Neuron | Class | 1 | 2 | 3 | 4 | 5 |
| ddaB | Alpha | 2 | 8 | 29 | 112 | 0 |
| ddaB | Alpha | 2 | 7 | 32 | 130 | 0 |
| vmd1 | Alpha | 2 | 6 | 20 | 85 | 0 |
| ddaC | Beta | 2 | 6 | 17 | 71 | 262 |
| ddaC | Beta | 2 | 5 | 15 | 55 | 220 |
| ddaD | Gamma | 2 | 4 | 20 | 84 | 332 |
| ldaC | Gamma | 2 | 8 | 22 | 82 | 299 |
| vdaB[2] | Gamma | 1 | 4 | 13 | 53 | 184 |

[1]The dendritic arbor of each neuron was reconstructed from a series of confocal micrographs taken from Lucifer yellow fills. Montaged images were analyzed directly using a computer by color coding and counting each branch. Neurons listed twice correspond to data taken from two different cell fills.
[2]The lower complexity of vdaB is correlated with a smaller overall area of innervation, comparable in size to that of vmd1.

## Peripheral dendritic arbors of the remaining dorsal, lateral, and ventral da neurons

The distinct dendritic morphologies seen among the dorsal cluster of da neurons led us to examine the branching patterns of the remaining da neurons. Each neuron that we examined shared clear morphological features with one of the three "archetypal" dorsal neurons. We, therefore, segregate the da neurons into three classes, termed the *alpha*, *beta*, and *gamma* classes, represented by ddaB, ddaC, and ddaD, respectively.

The dendrites of vmd1 resembled those of ddaB, and we place these two neurons in the alpha class (Fig. 6). vmd1 Showed fewer higher order branches, and many of these were merely short protrusions (Fig. 6). Neither ddaB nor vmd1 showed the dendritic varicosities seen in other da neurons (Adams et al., 1998; Grueber and Truman, 1999). vmd1 Innervated only the anterior ventral half of each

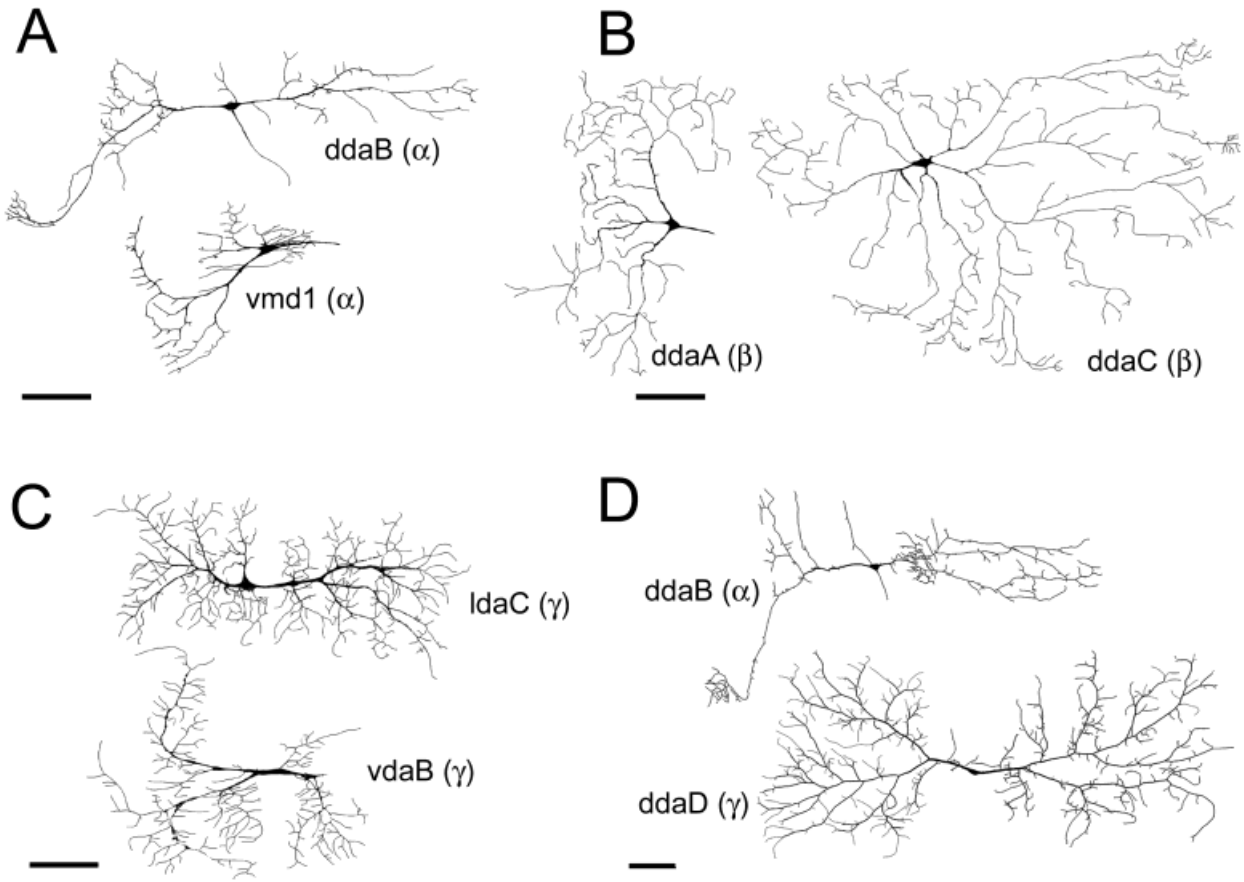


Fig. 6. Tracings of the dendritic branching of various dendritic arborization (da) neurons in first (A–C)- and second (D)-instar larvae. **A:** The alpha neurons ddaB and vmd1 both have relatively sparsely branched dendrites, although branching may be locally very high (as in the anterior most domain of ddaB). **B:** The beta neurons, including ddaC and ddaA, have long and thin dendritic branches that may cover relatively large areas of the epidermis. **C:** ldaC and vdaB, in addition to ddaD (see Fig. 5C), belong to the gamma class, having highly organized dendritic fields, with a characteristic dense innervation of each annulus. **D:** The morphologies of ddaB, an alpha neuron, and ddaD, a gamma neuron, in the second-instar larva. Anterior is to the left. Scale bars = 100 μm.

hemisegment (n = 5; Fig. 6), a region distinct from that innervated by ddaB. The dendrites of bilaterally homologous vmd1 neurons met at the ventral midline but did not overlap with each other (data not shown). Thus, the dendrites of the alpha neurons have completely nonoverlapping projections. ddaB and vmd1 showed the lowest dendritic complexity of any of the da neurons (Table 1).

In addition to ddaC (Fig. 5B), the beta cells consist of ddaA (Fig. 6) and vdaC. Two additional neurons ($ldaA_1$ and vdaD) may also belong to this class; however, fills of these less accessible ventral and lateral cells were partial and, therefore, only marginally informative. ddaA had a morphology that was similar to ddaC, in that it had long and sinuous midorder branches. Its dendrites spread toward the anterior region of the segment, away from the dendrites of ddaC, and crossed into the last annulus of the next anterior segment. These neurons showed a greater dendritic complexity than the dendrites of ddaB or vmd1 (Table 1).

The gamma neurons include ddaD as well as ldaC, vdaB, and vdaA (Fig. 6). Two other neurons, ldaB and $ldaA_2$, may also belong to this group, but fills of these lateral cells were only partial and did not reveal their full morphology. Each gamma neuron shared several features with ddaD, including higher order branches that avoid crossing, and terminating near, annular borders (Fig. 6). These neurons also had a higher branch complexity than either the alpha or the beta neurons (Table 1). The morphological similarity between members of this class is best exemplified by ddaD and ldaC, two neighboring neurons in the dorsal region of each hemisegment (cf. Figs. 5C and 6). Both neurons have approximately the same area of innervation (except that ldaC extends only a single branch into annulus 1), a similar dendritic complexity (Table 1), and a similar pattern of primary branch outgrowth. Other gamma cells such as vdaB and vdaA had smaller areas of innervation but appeared also to recognize and avoid annular borders.

The dendrites of both ddaB (alpha class) and ddaD (gamma class) grew substantially between hatching and the second larval stage (n = 5). For example, the length of ddaD expanded from approximately 0.65 mm at hatching to 1.1 mm early in the second larval stage (Fig. 6D). However, the regions of the segment that were innervated by ddaB (limited regions of the dorsal body wall) and ddaD (the entire dorsal half of the dorsal body wall) were the same in the first two larval instars (Fig. 6D). Importantly, the distinct dendritic morphologies that we observed in the various classes of da neurons in first-instar larvae were also evident in later instars. Consequently, they are characteristics of the mature sensory neurons and not transient developmental states.

## Central projections of representative alpha, beta, and gamma neurons

Our LY fills indicated that the da system comprises distinct morphological classes. We suspected that cells in the same class might be united by their physiological function; however, we could not directly test this idea, because most of the da neurons are inaccessible for electrophysiological analysis. We, therefore, examined whether the axonal projections of neurons in the same class show similar types of central arborizations. The region of the CNS to which insect sensory neurons project is correlated with their function (Pflüger et al., 1988). The

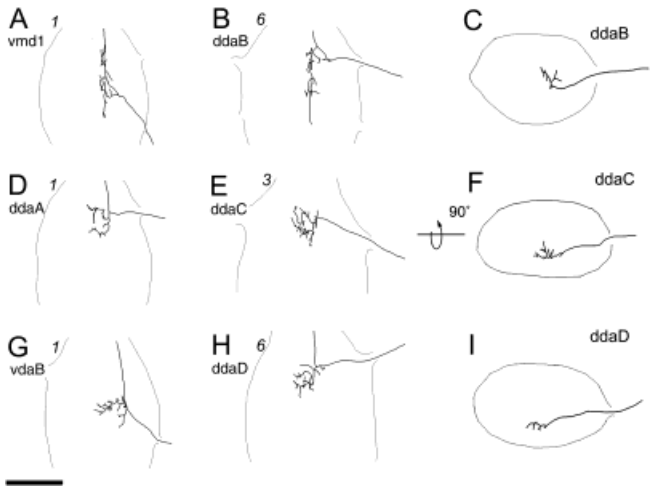


Fig. 7. Central projections of representative dendritic arborization (da) neurons in first-instar larvae as revealed by Lucifer yellow filling and confocal microscopy. The central projections of the alpha neurons vmd1 (**A**) and ddaB (**B**) do not cross the midline, send a projection to the next anterior ganglion, and have an intermediate projection (**C**). The central projections of the beta neurons ddaA (**D**) and ddaC (**E**) cross the midline and, with the possible exception of a single branch of ddaC, are restricted to the very ventral neuropil (**F**). Betweem these two, only ddaA, a neuron located more anteriorly on the body wall, projects to the ipsilateral connective. The gamma neurons vdaB (**G**) and ddaD (**H,I**) have ventral branches that extend into the contralateral neuropil. vdaB branches immediately upon entering the neuropil, whereas ddaD projects nearly to the midline before sprouting begins. Both cells project into the ipsilateral longitudinal connective. Numbers of observations are shown at upper left. The neuropil is indicated by a gray line. Anterior is upward for the first two columns; dorsal is upward for the last column. Scale bar = 50 μm.

axons of tactile receptors and chemoreceptors typically terminate in the ventral neuropil (Levine et al., 1985; Pflüger et al., 1988; Murphey et al., 1989; Nottebohm et al., 1992). Proprioceptors, on the other hand, usually project to more dorsal neuropil (Pflüger et al., 1988). We observed two distinct types of axonal projections among the da neurons (Fig. 7). The axons of vmd1 (n = 1; Fig. 7A) and ddaB (n = 6; Fig. 7B), the two alpha class neurons, projected into the ventral neuropil but abruptly turned near the midline and projected to an intermediate region of the neuropil (Fig. 7C). These axons did not cross the midline of the CNS, but both had collaterals that extended to the next anterior ganglion. In contrast to the alpha neurons, the projections of the beta and gamma neurons ddaA (n = 1), ddaC (n = 3), vdaB (n = 1), and ddaD (n = 6) were restricted to the ventral neuropil (Fig. 7). Each had branches that crossed the midline to the contralateral neuropil. ddaA, ddaD, and vdaB extended an axon collateral into the anterior ipsilateral connective, but our fills did not allow us to follow them into the next anterior ganglion. We did not observe any projections to more posterior ganglia. The central projections of the remaining neurons could not be determined, because the dissection required to expose their cell bodies usually severed the axons. By virtue of these projection patterns, the sensory information received from the alpha neurons is likely processed in the CNS differently from that received from the beta and gamma neurons.

### Tiling of the body wall by neurons of the same class

In some sensory systems, such as the mammalian retina, functionally similar neurons innervate nonoverlapping regions of a planar receptive area (Wässle et al., 1981). Our single-cell fills led us to suspect that a similar phenomenon might occur in the da system. To test this idea further, we filled specific pairs of da neurons to examine patterns of dendritic overlap between different cells (*heteroneuronal* overlap). Double fills of ddaA and ddaC (n = 4), two beta neurons, showed that their dendrites often meet, but they avoid overlapping in all but a few cases (Fig. 8A,B; a single overlap was consistently observed just dorsal to the sensory hair innervated by desB; nomenclature according to Grueber and Truman, 1999). By contrast, the dendrites of ddaC overlapped extensively with ddaB, an alpha neuron (n = 7; Fig. 9A), and ddaD and ldaC (both gamma neurons; data not shown). These data suggest that beta neurons are selectively excluded from each other's dendritic fields. Based on the position and dendritic arbors of the remaining beta neurons, these cells together appear to tile the entire epidermis (Fig. 10).

We also examined the gamma neurons. A double fill of ddaD and ldaC (n = 1) showed that their dendrites meet within the boundaries of each annulus but do not overlap (Fig. 8C,D). The difficulty of filling ldaC prevented additional double fills, so this observation was confirmed by analyzing numerous cGMP immunostains of these da neurons (data not shown). In contrast to the lack of overlap between ddaD and ldaC, the dendrites of ddaD showed extensive overlap with dendrites of ddaB (an alpha class neuron; Fig. 9B,C) and ddaC and ddaA (beta class neurons; data not shown). Pairwise dye fills could not be performed for the remaining gamma neurons; however, the spacing of their cell bodies and the shapes of their dendritic arbors as revealed by single-cell fills suggest that the dendrites of the gamma cells are largely nonoverlapping and tile the entire epidermis (Fig. 10).

In summary, the three classes of identifiable da neurons partition the segment in different ways (Fig. 10). The alpha neurons (vmd1 and ddaB) have arbors concentrated primarily along the anterior margin of the segment. By contrast, the beta (vdaC, vdaD, $ldaA_1$, ddaA, and ddaC) and the gamma (vdaA, vdaB, $ldaA_2$, ldaC, ddaD, and ldaB) da neurons both appear to tile the entire segment, forming two independent maps of the body surface (Fig. 10). Although the secondary plexus neurons (Grueber and Truman, 1999) are not treated here, this population of neurons appears to provide another complete layer of tiling in first-instar larvae (W.B.G. and J.W.T., unpublished data).

## DISCUSSION

### Dendritic arborization neurons have distinct physiological responses

The physiological roles of larval da neurons have not previously been examined, probably because the cell bodies are buried beneath the body wall musculature and are relatively inaccessible for electrophysiological analysis. Our recordings from a group of dorsal da neurons clearly show that different cells have distinct sensory responses (Fig. 3). This finding generally agrees with the earlier studies of Anderson and Finlayson (1978), who showed that ventral body wall neurons in adult tsetse flies have distinct basal firing patterns, stimulus-response properties, and poststimulus recovery characteristics. However, because their study focused on a different organism, a different developmental stage, and a different region of the body wall, few broad conclusions can as yet be made about the role of the subepidermal system. Both their study and ours identify a type of neuron that shows a high basal frequency and adapts slowly to tonic stimuli (ddaB in *Manduca* and the f, g, or h cell in tsetse flies) and could, therefore, sense long-term changes in body size (Fig. 3). In the tsetse fly, such neurons were proposed to detect body wall distension during blood feeding (Anderson and Finlayson, 1978). In *Manduca* larvae also, ddaB could monitor body size, with the information perhaps interacting with proprioceptive or molt-inducing pathways. The possibility of such a role for ddaB is particularly intriguing given that one of its dendritic arbors fans out to cover an anterior fold (Fig. 5A). This might allow ddaB to sense local changes in the topography of this patch of cuticle. A sense of body size could derive in part or whole from the monitoring of such restricted body regions.

Other *Manduca* da neurons, such as ddaD, are likely involved in the reception of forceful tactile stimuli. ddaD showed low-level sporadic activity and responded to moderately intense punctate stimuli delivered to the cuticle (Fig. 3). This neuron showed its highest activity during periods of stimulus application and withdrawal and may, therefore, encode stimulus velocity, similarly to the leech T cells (Nicholls and Baylor, 1968; Carlton and McVean, 1995). It will be important to characterize further the relative contribution of stimulus velocity and stimulus intensity to the sensory response of ddaD. Interestingly, the response of caterpillars to stimulation of the cuticle can range from slight bending to violent thrashing (Frings, 1945; Walters et al., 2001; W.B.G. and J.W.T., unpublished observations). We suspect that activity from ddaD, as well as from other da neurons, including ddaC, contributes to this behavioral repertoire. However, we do not know the response characteristics of ddaC, because we were unable to identify an extracellular unit associated with this cell. Because this neuron has a relatively thin axon, spikes may have been too small to resolve above the noise in our recordings. Alternatively, ddaC could respond preferentially to stimuli different from those we delivered to the body wall, such as more noxious stimuli. Studies of *Drosophila* da neurons have indicated that a group of the cells may participate in the behavioral response to noxious heat (W.D. Tracey & S. Benzer, pers. comm.). It is therefore conceivable that some da neurons in *Manduca*, perhaps including ddaC, function as nociceptors.

### Functionally distinct neurons belong to distinct morphological classes

Our morphological analysis of *Manduca* da neurons indicates that they comprise at least three distinct types of sensory cells, which we have termed the *alpha*, *beta*, and *gamma* classes (Fig. 6; Table 2). This grouping is based on peripheral dendrite morphology, specifically the complexity of arbors and the shapes of particular branches. Because dorsal cells shown to have distinct sensory responses (Fig. 3) belong to different morphological classes, our groupings likely reflect functional categories of da neurons.

Additional evidence for such functional classes derives from the axonal projections made by da neurons (Fig. 7). The dorsoventral positioning of sensory axon terminals determines the identities of their central synaptic partners and consequently influences how afferent sensory information is processed (Pflüger et al., 1988). We have found that cells within the same da class project to the same layer of the central neuropil. Beta and gamma neurons project to the ventral neuropil (Fig. 7F,I) in a pattern similar to tactile bristles (Levine et al., 1985). We do not know whether each type of neuron (beta, gamma, and bristle) arborizes in the same region of the ventral neuropil. The axons of beta and gamma neurons that we filled either were restricted to a single neuropil or projected to anterior ganglia. With only two exceptions, this is also the projection pattern of bristle afferents found on the abdomen of newly hatched *Manduca* (Levine et al., 1985). The

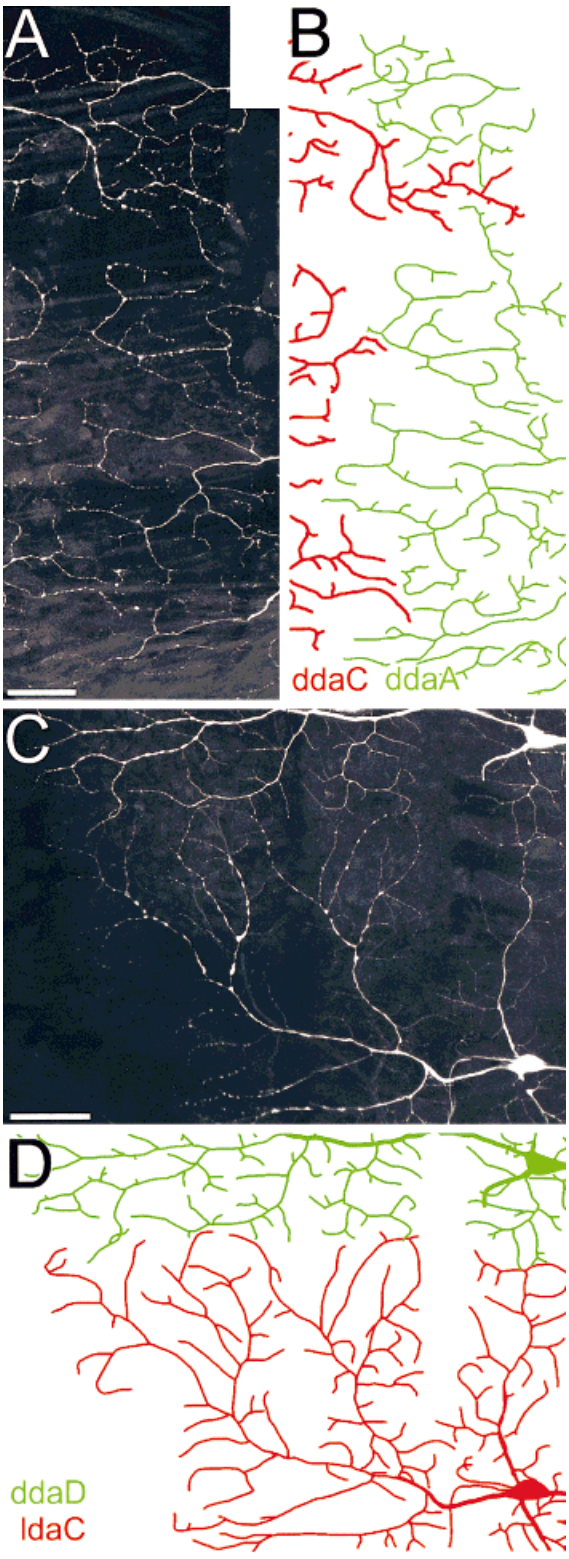


Fig. 8. Dendritic fields of dendritic arborization (da) neurons belonging to the same class do not overlap. Pairs of cells were filled with Lucifer yellow (LY) and reconstructed as montages from several confocal images, and the dendrites were outlined and pseudocolored to aid in visualization. **A,B:** The dendrites of ddaA (originating in the next posterior segment; green in B) and ddaC (red in B), both beta neurons, form a nonoverlapping boundary where they meet. **C,D:** Similarly, two members of the gamma class, ldaC (red in D) and ddaD (green in D), avoid each other's dendritic fields. Scale bars = 50 μm.

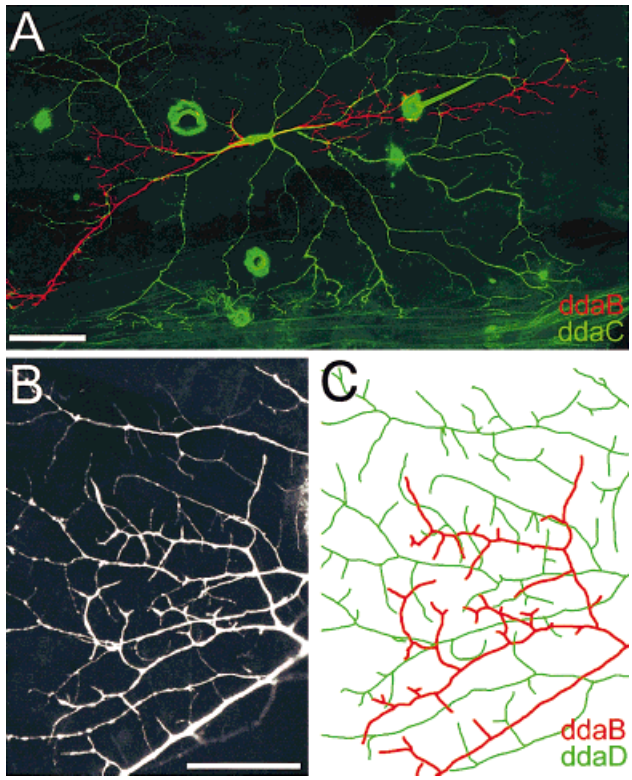


Fig. 9. Dendritic fields of dendritic arborization (da) neurons in different classes overlap extensively. **A:** ddaB (alpha class; red) and ddaC (beta class; green) have overlapping dendrites. Terminal branches do not avoid those belonging to the other cell. The image of ddaC is the same as that presented in Figure 5B. **B,C:** ddaB (alpha class; red in C) and ddaD (gamma class; green in C) overlap over much of their dendritic field. Shown is the region just anterior to desB, a sensory bristle whose autofluorescent socket can just be seen in the far right area of B. Anterior is to the left. Scale bars = 100 μm in A, B, 50 μm in B (applies to B,C).

alpha neurons had a strictly ipsilateral termination in intermediate neuropil, a pattern that was distinct from the projections of bristles and beta and gamma neurons (Fig. 7C). The alpha neuron projections are anatomically similar to those of *Drosophila* chordotonal organs, which project to a midventral region of the ipsilateral neuropil (Schrader and Merritt, 2000). The projection pattern that we see for the alpha neurons, therefore, supports our hypothesis that these neurons have a proprioceptive function.

The classes of da neurons also differ in their regulation of cGMP signaling pathways. Previous studies in *Manduca* have shown that different da neurons exhibit distinct patterns of cGMP production (Grueber and Truman, 1999). Most neurons produce cGMP when stimulated by exogenous NO, although a few show an EGTA-stimulated cGMP production (Grueber and Truman, 1999; W.B.G. and J.W.T., unpublished data). The cells that show these distinct patterns are in different functional classes. Cells that show NO-dependent increases correspond to the beta and gamma classes. The alpha neurons, on the other hand, are those that exhibit $Ca^{2+}$-sensitive cGMP production.

## Developmental implications of tiling and dendritic field organization

Each of the da neurons had a highly stereotyped dendritic morphology and defined dendritic field. We find that dendrites of da neurons belonging to different classes can overlap extensively, but those of neurons in the same class (i.e., the beta neurons ddaA and ddaC or the gamma neurons ldaC and ddaD) form nonoverlapping boundaries where they meet (Fig. 8). A lack of overlap was also observed where the dendritic fields of homologous cells meet at the dorsal and ventral midlines (data not shown). Our data therefore indicate that the beta and gamma classes separately provide a complete tiling of the body wall and the alpha neurons provide a partial coverage of the body wall.

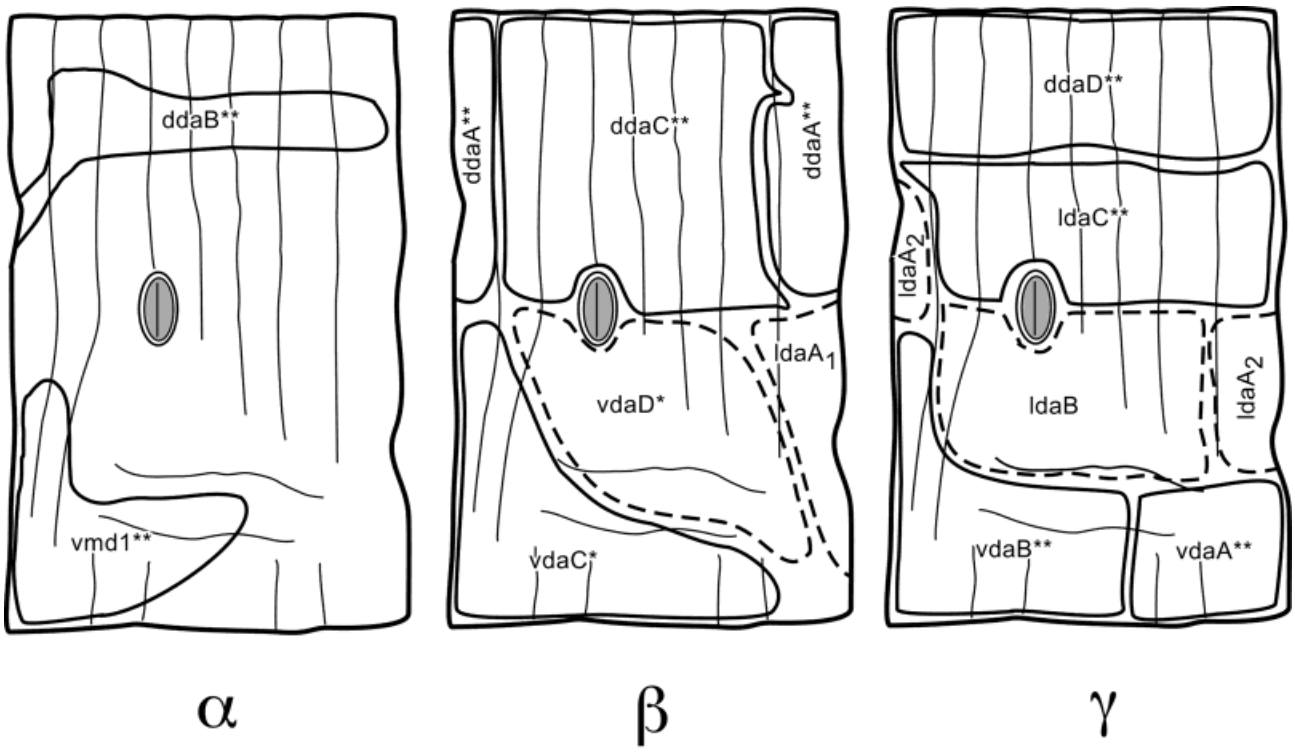


Fig. 10. Schematic representation of the dendritic areas of alpha (α), beta (β), and gamma (γ) dendritic arborization (da) neurons in the second abdominal segment (A2). Cells that were impaled and filled three or more times are indicated by a double asterisk. Cells filled fewer than three times are indicated by a single asterisk. The possible class memberships and dendritic territories of the remaining cells (dashed outlines) are based on cGMP stains and/or a partial fill of the cell.

TABLE 2. Morphological and Functional Properties of *Manduca* da Neurons

| Class | Example | Complexity[1] | Central projection[2] | Putative function | Body wall innervation[3] |
|---|---|---|---|---|---|
| Alpha | ddaB | Low | Intermediate | Proprioceptor | Partial |
| Beta | ddaC | Intermediate/high | Ventral | ? | Complete |
| Gamma | ddaD | High | Ventral | Exteroreceptor/touch receptor | Complete |

[1]The relative dendritic complexity was determined by Strahler analysis.
[2]The classes project to either the ventral neuropil or the intermediate neuropil.
[3]Based on the demonstrated degree of innervation of the dorsal body wall and the distribution of other putative class members in the case of beta and gamma classes. Innervation is nonredundant within each class. The beta and gamma classes, but not the alpha class, appear to innervate the entire body wall of the larva.

One mechanism for the beta and gamma classes to partition the body wall in such a manner could involve local dendritic interactions that cause processes to avoid each other during development. Such interactions are thought to prevent overlap among functionally similar types of mammalian retinal ganglion cells (Wässle et al., 1981; Amthor and Oyster, 1995; Weber et al., 1998) and also to influence the territories innervated by leech somatosensory neurons (Blackshaw et al., 1982; Gan and Macagno, 1995). Dendritic competition between a pair of bilaterally homologous dorsal da neurons has been observed in *Drosophila* and appears to require proper levels of Flamingo, a protocadherin family member (Gao et al., 2000). Given our data showing that tiling occurs not only among homologous cells but also independently among members of the same class, it is likely that each class of neurons uses different signaling molecules to establish dendritic domains.

Mechanisms other than heteroneuronal avoidance also likely contribute to the characteristic dendritic architectures of the da neurons. Isoneuronal (same cell) interactions would produce a fairly even spacing of dendritic branches, such as that seen for all da neurons (Fig. 6). Functionally, such interactions would ensure that each cell achieves a maximal coverage of its receptive field (Kramer and Kuwada, 1983). Additionally, for the gamma neurons, higher order dendritic branches are confined to discrete segmental annuli and fail to terminate within a zone immediately adjacent to annular borders (Fig. 5C). The dendrites of da neurons may, therefore, receive at least three types of extrinsic instructive signals during development, arising from the following: 1) interactions with branches of other like neurons, 2) interactions with the branches of the same neuron, and 3) interactions with the epidermis or basement membrane of each annulus. Because the different classes of neurons have distinct dendritic morphologies and highly specific patterns of dendritic avoidance, the molecular nature of these signals is likely different for each class.

### Evidence for distinct classes of da neurons in other insects

The *Drosophila* PNS is an important model for developmental and functional studies, so it is instructive to compare our results in *Manduca* to what is known for flies. The PNS of *Manduca* consists of approximately the same numbers of da neurons (the primary plexus neurons; Grueber and Truman, 1999) as are seen in *Drosophila* larvae (Bodmer and Jan, 1987). The axonal projections made by *Drosophila* da neurons are similar to those of *Manduca*. In *Drosophila*, most axons terminate in the ventral neuropil except for those of the ventral neuron vpda and another neuron in the dorsal body wall (Merritt and Whitington, 1995). Both of these cells project to more intermediate neuropil, and at least vpda has a strictly ipsilateral projection (Schrader and Merritt, 2000), similarly to the two alpha neurons that we identify in *Manduca*. The peripheral dendritic morphologies of individual *Drosophila* da neurons are not yet established, so a direct comparison with *Manduca* is not possible at this time. Nevertheless, these data together suggest that flies, like *Manduca*, have multiple distinct types of da neurons.

With the *Drosophila* system as a developmental model, we can ask how the morphological and functional classes of da neurons could relate to their developmental origin. The various *Drosophila* da neurons originate from different types of lineages and require different genes for their specification. Most of the neurons are lineally related to external sensory bristles (md-es neurons; Brewster and Bodmer, 1995; Orgogozo et al., 2001) or arise alone (solo-md neurons). md-es neurons and some solo-md neurons require proneural genes in the *achaete-scute* complex (ASC; Dambly-Chaudiere and Ghysen, 1987; Brewster and Bodmer, 1995). vpda, by contrast, requires *atonal* expression (Jarman et al., 1993), whereas small numbers of solo-md neurons require *amos* (Huang et al., 2000). Our data from *Manduca* show that beta and gamma neurons have central projections that are restricted to the ventral neuropil, similarly to the ASC-dependent *Drosophila* neurons, but have distinct dendritic morphologies in the periphery. We, therefore, speculate that beta and gamma neurons are homologous with subgroups of ASC-dependent *Drosophila* da neurons. The alpha neurons, on the other hand, are likely homologs of the *Drosophila* da neurons that require *atonal*. To determine the relationship between the developmental categories of da neurons and the morphological and functional classes that we have characterized, it will be important to examine the branching patterns and physiology of individual da neurons in *Drosophila*.

## ACKNOWLEDGMENTS

We thank members of the Graubard and O'Carroll laboratories and Dr. David Baldwin for helpful advice on electrophysiology and dye filling, Dr. Michael Tu for assistance with the calibration of von Frey filaments, and Dr. John Kuwada for anti-LY. We thank Drs. Lynn Riddiford and Anhthu Hoang, as well as anonymous reviewers, for their helpful comments on the manuscript, and W.D. Tracey and S. Benzer for communicating results prior to publication.

## LITERATURE CITED

Adams CM, Anderson MG, Motto DG, Price MP, Johnson WA, Welsh MJ. 1998. Ripped pocket and pickpocket, novel *Drosophila* DEG/ENaC subunits expressed in early development and mechanosensory neurons. J Cell Biol 140:143–152.

Amthor FR, Oyster CW. 1995. Spatial organization of retinal information about the direction of image motion. Proc Natl Acad Sci USA 92:4002–4005.

Anderson M, Finlayson LH. 1978. Topography and electrical activity of peripheral neurons in the abdomen of the tsetse fly (*Glossina*) in relation to abdominal distension. Physiol Entomol 3:157–167.

Beck JC, Murray JA, Willows AO, Cooper MS. 2000. Computer-assisted visualizations of neural networks: expanding the field of view using seamless confocal montaging. J Neurosci Methods 98:155–163.

Bell RA, Joachim FA. 1976. Techniques for rearing laboratory colonies of tobacco hornworms and pink bollworms. Ann Entomol Soc Am 69:365–373.

Berry M, Hollingsworth T, Anderson EM, Flinn RM. 1975. Application of network analysis to the study of the branching patterns of dendritic fields. Adv Neurol 12:217–245.

Blackshaw SE. 1981. Morphology and distribution of touch cell terminals in the skin of the leech. J Physiol 320:219–228.

Blackshaw SE, Nicholls JG, Parnas I. 1982. Expanded receptive fields of cutaneous mechanoreceptor cells after single neuron deletion in the leech central nervous system. J Physiol 326:261–268.

Bodmer R, Jan YN. 1987. Morphological differentiation of the embryonic peripheral neurons in *Drosophila*. Rouxs Arch Dev Biol 196:69–77.

Brewster R, Bodmer R. 1995. Origin and specification of type II sensory neurons in *Drosophila*. Development 121:2923–2936.

Carlton M, McVean A. 1995. The role of touch, pressure, and nociceptive mechanoreceptors of the leech in unrestrained behavior. J Comp Physiol A177:781–791.

Dambly-Chaudiere C, Ghysen A. 1987. Independent subpatterns of sense organs require independent genes of the *achaete-scute* complex in *Drosophila* larvae. Genes Dev 1:297–306.

Darboux I, Lingueglia E, Pauron D, Barbry P, Lazdunski M. 1998. A new member of the amiloride-sensitive sodium channel family in *Drosophila melanogaster* peripheral nervous system. Biochem Biophys Res Commun 246:210–216.

Frings H. 1945. The reception of mechanical and thermal stimuli by caterpillars. J Exp Zool 99:115–139.

Gan W-B, Macagno ER. 1995. Interactions between segmental homologs and between isoneuronal branches guide the formation of sensory terminal fields. J Neurosci 15:3243–3253.

Gao F-B, Kohwi M, Brenman JE, Jan LY, Jan YN. 2000. Control of dendritic field formation in *Drosophila*: the roles of Flamingo and competition between homologous neurons. Neuron 28:91–101.

Grueber WB, Truman JW. 1999. Development and organization of a nitric oxide-sensitive peripheral neural plexus in larvae of the moth, *Manduca sexta*. J Comp Neurol 404:127–141.

Huang M-L, Hsu C-H, Chien C-T. 2000. The proneural gene *amos* promotes multiple dendritic neuron formation in the *Drosophila* peripheral nervous system. Neuron 25:57–67.

Jarman AP, Grau Y, Jan LY, Jan YN. 1993. *atonal* is a proneural gene that directs chordotonal organ formation in the *Drosophila* peripheral nervous system. Cell 73:1307–1321.

Kramer AP, Kuwada JY. 1983. Formation of the receptive fields of leech mechanosensory neurons during embryonic development. J Neurosci 3:2474–2486.

Levine RB, Truman JW. 1985. Dendritic reorganization of abdominal motoneurons during metamorphosis of the moth, *Manduca sexta*. J Neurosci 5:2424–2431.

Levine RB, Pak C, Linn D. 1985. The structure, function, and metamorphic reorganization of somatotopically projecting sensory neurons in *Manduca sexta* larvae. J Comp Physiol A157:1–13.

Merritt DJ, Whitington PM. 1995. Central projections of sensory neurons in the *Drosophila* embryo correlate with sensory modality, soma position, and proneural gene function. J Neurosci 15:1755–1767.

Miyazaki S. 1980. The ionic mechanism of the action potentials in neurosecretory cells and nonneurosecretory cells of the silkworm. J Comp Physiol 140:43–52.

Murphey RK, Possidente DA, Pollack G, Merritt DJ. 1989. Modality-specific axonal projections in the CNS of the flies *Phormia* and *Drosophila*. J Comp Neurol 290:185–200.

Nicholls JG, Baylor DA. 1968. Specific modalities and receptive fields of sensory neurons in the CNS of the leech. J Neurophysiol 31:740–756.

Nottebohm E, Dambly-Chaudiere C, Ghysen A. 1992. Connectivity of chemosensory neurons is controlled by the gene *poxn* in *Drosophila*. Nature 359:829–832.

Orgogozo V, Schweisguth F, Bellaïche Y. 2001. Lineage, cell polarity, and *inscuteable* function in the peripheral nervous system of the *Drosophila* embryo. Development 128:631–643.

Perry VH, Linden R. 1982. Evidence for dendritic competition in the developing retina. Nature 297:683–685.

Pflüger HJ, Braunig P, Hustert R. 1988. The organization of mechanosensory neuropils in locust thoracic ganglia. Phil Trans R Soc London 321:1–26.

Pinchon Y, Sattelle DB, Lane NJ. 1972. Conduction processes in the nerve cord of the moth *Manduca sexta* in relation to its ultrastructure and haemolymph ionic concentration. J Exp Biol 56:717–734.

Schrader S, Merritt DJ. 2000. Central projections of *Drosophila* sensory neurons in the transition from embryo to larva. J Comp Neurol 425:34–44.

Strahler AN. 1953. Revisions of Horton's quantitative factors in erosional terrain. Trans Am Geophysical Union 34:345.

Trimmer BA, Weeks JC. 1989. Effects of nicotinic and muscarinic agents on an identified motoneuron and its direct afferent inputs in larval *Manduca sexta*. J Exp Biol 144:303–337.

Uylings HBM, Smit GJ, Veltman WAM. 1975. Ordering methods in quantitative analysis of branching structures of dendritic trees. Adv Neurol 12:247–254.

Walters ET, Illich PA, Weeks JC, Lewin MR. 2001. Defensive responses of larval *Manduca sexta* and their sensitization by noxious stimuli in the laboratory and field. J Exp Biol 204:457–469.

Wässle H, Peichl L, Boycott BB. 1981. Dendritic territories of cat retinal ganglion cells. Nature 292:344–345.

Weber AJ, Kalil RE, Stanford LR. 1998. Dendritic field development of retinal ganglion cells in the cat following neonatal damage to visual cortex: evidence for cell class specific interactions. J Comp Neurol 390:470–480.

Weevers RdeG. 1966a. A lepidopteran saline: effects of inorganic cation concentration on sensory, reflex, and motor responses in a herbivorous insect. J Exp Biol 44:163–175.

Weevers RdeG. 1966b. The physiology of a lepidopteran muscle receptor I. The sensory response to stretching. J Exp Biol 44:177–194.